

Article

# Channel and Bit Adaptive Power Control Strategy for Uplink NOMA VLC Systems

Zhen-Yu Wang \* , Hong-Yi Yu and Da-Ming Wang

National Digital Switching System Engineering and Technological Research Center, Zhengzhou 450001, China; maxyucn@163.com (H.-Y.Y.); wdm\_wangdaming@163.com (D.-M.W.)

\* Correspondence: xxgcmayu@163.com; Tel.: +86-135-8989-2325

Received: 30 November 2018; Accepted: 3 January 2019; Published: 9 January 2019



**Abstract:** Non-orthogonal multiple access (NOMA) can be an effective solution to the limited bandwidth of light emitting diodes for visible light communication (VLC) systems to support multiuser communication. The current available works for NOMA VLC systems mainly concentrate on downlinks and the existing power allocation algorithms mainly focus on the channel state information and ignore the influence of transmitted signals. In this paper, we propose a channel and bit adaptive power control strategy for uplink NOMA VLC systems by jointly considering the channel state information and the transmission bit rate. Under this adaptive power control strategy, it is proved that the received signal at the photodiode (PD) receiver constitutes a sizeable pulse amplitude modulation constellation and low-complexity maximum likelihood detection is admitted. The simulation results indicate that our proposed adaptive power control strategy outperforms the gain ratio power allocation scheme, fixed power allocation scheme, and time division multiple access scheme.

**Keywords:** visible light communication (VLC); uplink non-orthogonal multiple access (NOMA); adaptive power control (APC); maximum likelihood (ML) detection

## 1. Introduction

With the rapid development of solid-state lighting technology, visible light communication based on light emitting diodes (LEDs) has attracted a lot of interest in research [1–6] due to its unique merits such as low cost, large bandwidth, high security, freedom from spectral licensing issue, easy implementation into existing infrastructure, etc. However, multiuser communication support for VLC systems has become a challenging topic due to the limited modulation bandwidth of the LEDs and thus, multiple access technologies have become an hot spot for research.

For multiple access technologies, it is known that the orthogonal multiple access (OMA) techniques [3,7–9] such as frequency division multiple access (FDMA), time division multiple access (TDMA), code division multiple access (CDMA), and orthogonal frequency division multiple access (OFDMA) have been widely studied in recent years in both radio frequency (RF) communications and VLC. However, these OMA schemes allocate the limited frequency, time, and code resources among multiple users and thus, these resources cannot be fully reused [10,11]. In addition, these OMA schemes cannot guarantee the unique identifiability of each user's signal when users are dense. Very recently, non-orthogonal multiple access (NOMA), as a promising candidate for 5G wireless networks [12–15], has also been proposed for VLC systems due to the fact the VLC experiences high signal-to-noise ratio (SNR) and the NOMA schemes outperform the orthogonal counterparts in that particular region. Different from these OMA schemes, NOMA enables multiple users to simultaneously utilize all the available frequency, time, and code resources by multiplexing all the users' signals in the power domain at the transmitter.

### 1.1. Related Work and Motivation

In VLC systems, as an effective solution to the limited bandwidth of LEDs, NOMA has drawn great attention in recent years to support multiuser communications [16–21]. In [16], the authors investigate the ergodic sum rate and coverage probability of downlink NOMA VLC system. In [17,19], the basic concept of NOMA VLC has been introduced in detail and the authors presented a fixed power allocation (FPA) strategy and a gain ratio power allocation (GRPA) strategy. In [20], the symbol error rate performance of NOMA VLC system is analyzed. In [21], the author proposed an optimal power control algorithm for downlink VLC systems. However, almost all the literatures focused on downlink NOMA VLC studies and the task is more challenging for uplink NOMA VLC systems since the transmission of all users is difficult to be coordinated. In addition, the existing works on power allocation algorithm mainly are concentrated on the influence of channel state information and ignored the transmitted signals, which leads to the inability to take full advantage of NOMA to achieve efficient communication for VLC systems.

### 1.2. Contributions

Indeed, motivated by the above-mentioned factors, in this paper, we jointly consider the influence of channel state information and transmission bit rate and propose a channel and bit adaptively power control (APC) strategy for uplink NOMA VLC systems. Since the received constellation at the photodiode (PD) receiver has a nice structure under our proposed APC strategy, we develop a low-complexity maximum likelihood (ML) demodulation and decoding algorithm. Simulation results show that our proposed APC strategy outperforms the GRPA, FPA, and TDMA schemes.

### 1.3. Paper Organization

The rest of this paper is organized as follows. The uplink NOMA VLC system model we considered is introduced in Section 2. In Section 3, we propose the channel and bit adaptive power control strategy for transmitter and develops a low-complexity ML demodulation and decoding algorithm for receiver. Simulation results of our proposed APC, GRPA, FPA, and TDMA schemes are presented and discussed in Section 4. In Section 5, we summarize this paper.

## 2. System Model

As shown in Figure 1, in this paper, we consider a multiple access VLC system with  $N$  LED transmitters and one PD receiver, which is equivalent to an uplink NOMA VLC system. The  $N$  LED transmitters transmit their messages simultaneously to the PD receiver by modulating the optical intensity according to the transmitted data and the PD receiver performs direct detection to extract each LED's signal. Since the transmitted signals in realistic communication systems are drawn from finite-alphabet constellations, as well as the fact the transmitted signals in VLC systems must be non-negative and real-valued, in this paper, we consider unipolar pulse amplitude modulation (UPAM) for each LED's transmitted signal.

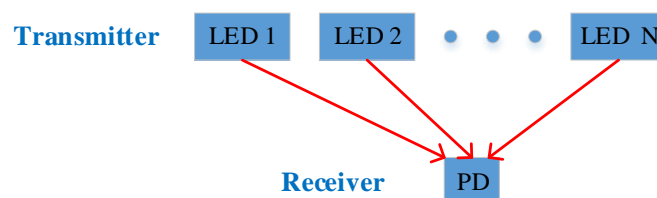


Figure 1. Multiple access system model.

We consider that the information-carrying signal from  $i$ -th LED to PD denoted by  $s_i$  is randomly, equally-likely and independently chosen from a  $2^{K_i}$ -ary UPAM constellation, i.e.,  $s_i \in \mathcal{S}_i = \{k\}_{k=0}^{2^{K_i}-1}$ , where  $K_i$  is the modulation order of UPAM. Then, let  $\gamma_i$  denote the power control factor ( $0 < \gamma_i \leq 1$ ) and thus, the received signal  $y$  at the PD receiver can be described as

$$y = \sum_{i=1}^N h_i \gamma_i s_i + \zeta \tag{1}$$

The receiver noise  $\zeta$  is mainly due to the shot noise and the thermal noise in VLC. The shot noise is mainly caused by the ambient light and the main source of ambient noise are sunlight and artificial light such as that of incandescent and fluorescent lamps [22,23]. Note that in the case where the blue light is used at the receiver for signal detection by narrow spectral filtering, the influence of ambient light is considerably reduced [24]. If the ambient light is negligible, then the dominant noise source is the receiver preamplifier thermal noise, which is signal independent and Gaussian [1,24]. Thus, in this paper, the noise  $\zeta$  is approximately modeled as additive white Gaussian noise (AWGN) with zero mean and variance  $\sigma^2$ . The parameter  $h_i$  denotes the channel coefficient between the PD receiver and the  $i$ -th LED transmitter. For VLC channels, the power of non-line-of-sight signals is much weaker than that of the line-of-sight (LOS) signals [25,26]. Thus, usually only LOS links are considered in VLC systems [16,17,20,26]. Then,  $h_i$  is determined by [1,25]

$$h_i = \begin{cases} \frac{(m+1)A}{2\pi d_i^2} \cos^m \phi_i T_s(\psi_i) g(\psi_i) \cos \psi_i, & 0 < \psi_i < \Psi, \\ 0, & \psi_i > \Psi. \end{cases} \tag{2}$$

where  $A$  is the effective detector area of PD,  $d_i$  depicts the distance between the PD receiver and the  $i$ -th LED transmitter,  $T_s(\psi_i)$  is the gain of the optical filter, and  $\Psi$  denotes the field-of-view angle of the PD receiver. In addition,  $\phi_i$  is the angle of emergence,  $\psi_i$  is the angle of incidence,  $m = \frac{-\ln 2}{\ln(\cos \Phi_{\frac{1}{2}})}$  with  $\Phi_{\frac{1}{2}}$  being defined the LED transmitter's half-power angle, and  $g(\psi_i)$  represents the gain of the optical concentrator given by

$$g(\psi_i) = \begin{cases} \frac{n^2}{\sin^2 \Psi}, & 0 < \psi_i < \Psi, \\ 0, & \psi_i > \Psi. \end{cases} \tag{3}$$

with  $n$  being the corresponding refractive index.

In this paper, we assume that the PD receiver receives all the users' signals at the same time and treat all the signals as useful signal components instead of noises. In addition, due to the relatively slow movement of people and fixed objects within a room, the channel can effectively be considered as time invariant and the channel state information can be easily obtained by training symbols and sent back to the transmitter periodically through uplink [24,27,28]. Therefore, in this paper, we ignore the influence of the asymmetry of the optical wireless links [29–32] and assume that the channel coefficients are fully available at the LED transmitters and the PD receiver. Without loss of generality, we rearrange the all channel coefficients and the sorted channel coefficients are given as follows.

$$h_1 \leq h_2 \leq \dots \leq h_i \leq \dots \leq h_N \tag{4}$$

### 3. Adaptive Power Control Strategy for Uplink NOMA VLC

In this section, to manage the multiuser interference and achieve efficient communication, we first propose an efficient channel and bit adaptive power control strategy which has a favorable property about the structure of the received constellation. Then, thanks to the nice constellation structure of the received signals, we develop a low-complexity demodulation and decoding algorithm for signal detection.

#### 3.1. Channel and Bit Adaptive Power Control

In NOMA-based systems, different power values are allocated to the users and the power control strategy is a key factor affecting the system's performance. In [28], we proposed an optimal power control strategy for two-user multi-access VLC system under the assumption that the two users' transmission bit rates are identical. In this paper, for multiuser communication scenarios with different

transmission bit rate of each user, we develop an efficient channel and bit adaptive power control strategy by jointly considering the effect of channel state information and transmission bit rate. The efficient adaptive power control strategy we proposed is given in the following algorithm.

**Algorithm 1.** (Channel and Bit Adaptive Power Control) Let  $\check{\gamma}_i, i = 1, 2, \dots, N$  denote the channel and bit adaptive power control coefficient. Then, it can be determined in the following.

$$\begin{cases} \check{\gamma}_1 = \frac{1}{\max_{2 \leq i \leq N} \{1, 2^{\sum_{j=1}^{i-1} K_j} \frac{h_1}{h_i}\}}, \\ \check{\gamma}_i = 2^{\sum_{j=1}^{i-1} K_j} \frac{h_1}{h_i} \check{\gamma}_1, \quad i = 2, 3, \dots, N. \end{cases} \quad (5)$$

This algorithm indicates that the adaptive power control strategy we proposed is essentially channel and bit adaptive, it enables each LED transmitter to transmit its own sub-constellation with amplitude being adaptively adjusted, and it has the following favorable property.

**Property 1.** The sum signal  $g = \sum_{i=1}^N h_i \check{\gamma}_i s_i$  constitutes a  $2^{\sum_{i=1}^N K_i}$ -ary equally-spaced UPAM constellation since  $g/h_1 \check{\gamma}_1 = (\sum_{i=1}^N h_i \check{\gamma}_i s_i)/h_1 \check{\gamma}_1 = s_1 + 2^{K_1} s_2 + \dots + 2^{\sum_{i=1}^{N-1} K_i} s_N \in \{k\}_{k=0}^{2^{\sum_{i=1}^N K_i} - 1}$ .

### 3.2. Low-Complexity Receiver Design

Intended for our proposed efficient adaptive power control strategy in the last subsection, in this subsection, our task is to develop an efficient detection algorithm for the receiver.

Let  $\check{D} = h_1 \check{\gamma}_1$ . Then, according to Property 1, the received signal  $y = \sum_{i=1}^N h_i \check{\gamma}_i s_i + \zeta$  can be rewritten by  $y = \check{D}(s_1 + 2^{K_1} s_2 + \dots + 2^{\sum_{i=1}^{N-1} K_i} s_N) + \zeta$ . Thus, we have the following low-complexity demodulation and decoding algorithm for signal detection.

**Algorithm 2.** (Fast ML Demodulation and Decoding) Let  $g \in \{\sum_{i=1}^N h_i \check{\gamma}_i s_i : s_i \in \mathcal{S}_i\}$  denote the sum signal. Then, the optimal ML estimate of  $g$  can be attained by

$$\hat{g} = \check{D} \times \begin{cases} 0, & \frac{y}{\check{D}} \leq 0 \\ \lfloor \frac{y}{\check{D}} + \frac{1}{2} \rfloor, & 0 < \frac{y}{\check{D}} \leq 2^{\sum_{i=1}^N K_i} - 1 \\ 2^{\sum_{i=1}^N K_i} - 1, & \frac{y}{\check{D}} > 2^{\sum_{i=1}^N K_i} - 1. \end{cases} \quad (6)$$

where  $y$  is the received signal and it is denoted by (1). Then, the estimate signal  $\hat{s}_i$  of  $s_i$  at the PD receiver is given as follows.

$$\begin{cases} \hat{s}_1 = \frac{\hat{g}}{\check{D}} \bmod 2^{K_1}, \\ \hat{s}_i = \frac{\frac{\hat{g}}{\check{D}} - \frac{\hat{g}}{\check{D}} \bmod 2^{\sum_{j=1}^{i-1} K_j}}{2^{\sum_{j=1}^{i-1} K_j}} \bmod 2^{K_i}, i \geq 2. \end{cases} \quad (7)$$

From Algorithm 2, we can find that our developed efficient detection algorithm is essentially a joint ML detection and thus, it is optimal for the sum signal detection. In addition, its computational complexity is much lower than conventional ML detection.

## 4. Simulations

In this section, we will carry out simulations to examine the performance of our proposed adaptive power control (APC) strategy for an equivalent uplink NOMA VLC system by comparing with GRPA, FPA, and TDMA schemes.

In this paper, we carry out the simulations in a 4.0 m × 4.0 m × 3.0 m room model for indoor environment, which is a typical simulation model in VLC systems [33–35]. As illustrated by Figure 2a,

the PD receiver is located at the ceiling and the LED transmitters are located at a plane with a height of 0.85 m, which is denoted by Receiver Plane. The other key system parameter settings according to [33–35] are illustrated by Table 1. The channel coefficients between the LED transmitters and the PD receiver can be computed based on (2) and without loss of generality, they are normalized by being divided by the maximum channel coefficient in our simulation. In addition, the SNR is defined by  $\frac{1}{\sigma^2}$  with the peak optical power being normalized. All the schemes to be compared are given as follows:

- (1) **Gain Ratio Power Allocation (GRPA)** [17]: The signal transmitted by the  $i$ -th LED is denoted by  $x_{GRPA_i} = P_i s_i$ , where  $P_i = (\frac{h_i}{h_1})^2 P_{i-1}$  and  $s_i \in \{k\}_{k=0}^{2^{K_i}-1}$ ,  $1 \leq i \leq N$ . In this simulation, we set  $P_1 = 1$ .
- (2) **Fixed Power Allocation (FPA)** [17,19]: The transmitted signal of LED  $i$  is denoted by  $x_{FPA_i} = F_i s_i$ , where  $F_i = \alpha F_{i-1}$  and  $s_i \in \{k\}_{k=0}^{2^{K_i}-1}$ ,  $1 \leq i \leq N$ . In this simulation, we set  $\alpha = 0.1$  and  $F_1 = 1$ .
- (3) **Time Division Multiple Access (TDMA)** [3]: With the successive  $N$  time slots, the transmitted signal of the  $N$  LEDs is given by  $\mathbf{x}_{TDMA} = [s_1, s_2, \dots, s_N]$ , where  $s_i \in \{k\}_{k=0}^{2^{N K_i}-1}$ ,  $1 \leq i \leq N$ .
- (4) **Adaptive Power Control (APC)**: Our proposed APC strategy is given in Algorithm 1.

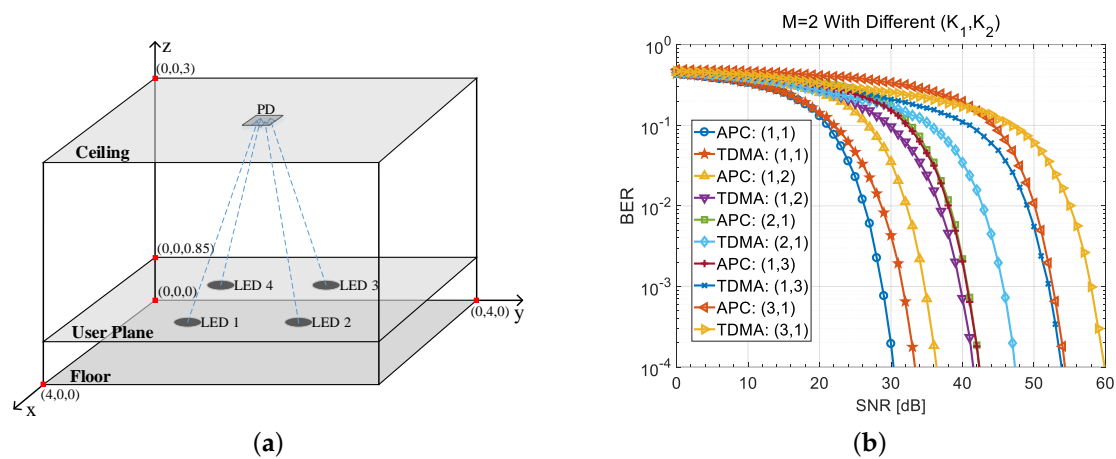


**Figure 2.** (a) Multiple access room model for simulation; (b) Two users’ BER performance comparisons of our proposed adaptive power control (APC) and time division multiple access (TDMA) for different  $(K_1, K_2)$ .

**Table 1.** Key System Parameters

Parameter	Value
Room size	4.0 m × 4.0 m × 3.0 m
PD detector area	$A = 1 \text{ cm}^2$
Field-of-view angle	$60^\circ$
Gain of optical concentrator	1.0
Half-power angle	$60^\circ$
Gain of optical filter	1.0
Height of user plane	0.85 m

In this paper, we simulate the users’ average BER performance of the above schemes for two LEDs, three LEDs, and four LEDs scenarios. For two LEDs scenario, the coordinates of the two LEDs are (1.0 m, 2.0 m, 0.85 m) and (3.0 m, 2.0 m, 0.85 m). For three LEDs scenario, the coordinates of the three LEDs are (1.0 m, 1.5 m, 0.85 m), (2.0 m, 3.0 m, 0.85 m), and (3.0 m, 1.5 m, 0.85 m). For four LEDs scenario, the coordinates of the four LEDs are (1.0 m, 1.0 m, 0.85 m), (1.0 m, 3.0 m, 0.85 m), (3.0 m, 3.0 m, 0.85 m), and (3.0 m, 1.0 m, 0.85 m). Since the obtained gains of our proposed design over other schemes at the error rate of  $10^{-4}$  have reached our expectations, the BER in all simulation figures are plotted up

to  $10^{-4}$  in this paper. In addition, the ML demodulator is adopted by all schemes to make all the comparisons fair and the simulations are detailed as follows.

#### 4.1. BER Performance Analysis for Stationary Locations

In this subsection, we simulate the BER performance of our proposed APC strategy and TDMA for given fixed PD's location.

We first evaluate the BER performance of our proposed APC over TDMA for different  $K_i$ . We consider that the coordinates of the PD receiver for two LEDs, three LEDs and four LEDs scenarios are (1.5 m, 2.0 m, 3.0 m), (1.5 m, 2.2 m, 3.0 m), and (1.5 m, 1.8 m, 3.0 m), respectively. The corresponding simulation results are illustrated by Figures 2b and 3a,b. Then, in order to obtain the BER performance of our proposed APC over TDMA for different PD's locations, for two LED transmitters scenario with  $K_1 = 1, K_2 = 3$ , we examine the BER performance of APC and TDMA for several fixed PD's locations and we show the simulation results in Figure 4a. From the above four figures, we can observe that the APC strategy we proposed significantly outperforms TDMA. This is mainly because the error performance of ML detection in high SNR region is dominated by the minimum Euclidean distance (MED) of the received constellation. By computations, the attained gain in terms of the ratio of MED of APC over TDMA is determined by

$$Gain = 20 \log_{10} \left( \frac{h_1 \check{\gamma}_1}{\sum_{i=1}^N 2^{K_i} - N} \right) / \left( \min_{1 \leq i \leq N} \frac{h_i}{2^{N K_i} - 1} \right) \quad (8)$$

For three LED transmitters scenario, for example,  $K_1 = 1, K_2 = 1, K_3 = 2$  and the PD receiver is located at (1.5 m, 2.2 m, 3.0 m). By computation based on (2), we can get that the value of the normalized and sorted channel coefficients are  $h_1 = 0.3942, h_2 = 0.7032, h_3 = 0.3942$  and then according to Algorithm 1, we have  $\check{\gamma}_1 = 0.4713, \check{\gamma}_2 = 0.5284, \check{\gamma}_3 = 1$ . Therefore, we can obtain that  $Gain = 20 \log_{10} \left( \frac{h_1 \check{\gamma}_1}{\sum_{i=1}^N 2^{K_i} - N} \right) / \left( \min_{1 \leq i \leq N} \frac{h_i}{2^{N K_i} - 1} \right) = 20 \log_{10} \left( \frac{0.3942 \times 0.4713}{2+2+2^2-3} \right) / \left( \frac{0.7431}{2^6-1} \right) \approx 9.97$  dB, which confirms with the simulation results in Figure 3a. For four LED transmitters scenario, for instance,  $K_1 = 1, K_2 = 1, K_3 = 2, K_4 = 2$  and the PD receiver is located at (1.5 m, 1.8 m, 0.85 m). According to (2) and Algorithm 1, we have  $h_1 = 0.3092, h_2 = 0.3786, h_3 = 0.5362, h_4 = 0.7032$  and  $\check{\gamma}_1 = 0.2842, \check{\gamma}_2 = 0.4643, \check{\gamma}_3 = 6557, \check{\gamma}_4 = 1$ . Then, we can get that  $Gain = 20 \log_{10} \left( \frac{h_1 \check{\gamma}_1}{\sum_{i=1}^N 2^{K_i} - N} \right) / \left( \min_{1 \leq i \leq N} \frac{h_i}{2^{N K_i} - 1} \right) = 20 \log_{10} \left( \frac{0.3092 \times 0.2842}{2+2+2+2^2-4} \right) / \left( \frac{0.7032}{2^8-1} \right) \approx 14.5$  dB, which is consistent with the simulation results in Figure 3b.

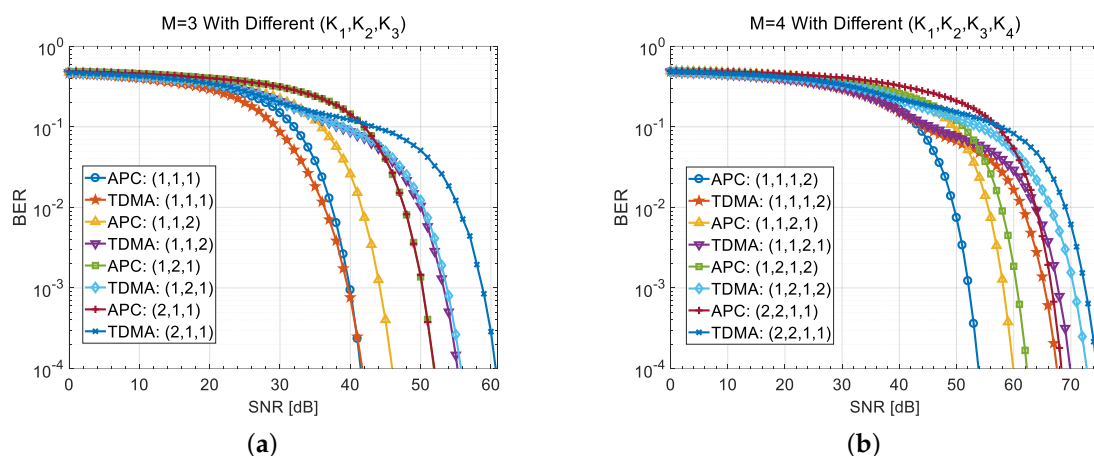


**Figure 3.** (a) Three users' BER performance comparisons of our proposed APC and TDMA for different  $(K_1, K_2, K_3)$ ; (b) Four users' BER performance comparisons of our proposed APC and TDMA for different  $(K_1, K_2, K_3, K_4)$ .

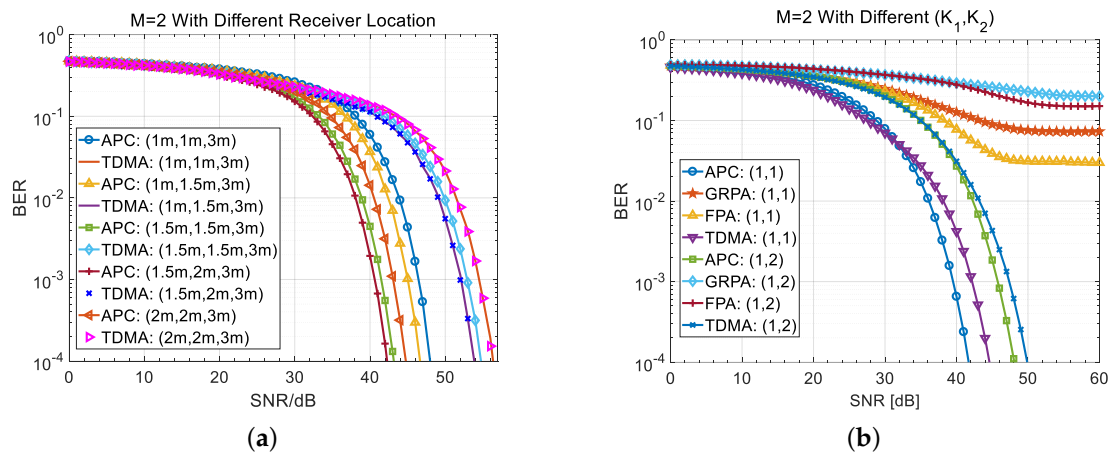


**Figure 4.** (a) Two users’ BER performance comparisons of our proposed APC and TDMA for different photodiode (PD) receiver’s location; (b) Two users’ average BER performance comparisons of our proposed APC, gain ratio power allocation (GRPA), fixed power allocation (FPA), and TDMA for different  $(K_1, K_2)$ .

#### 4.2. BER Performance Analysis for Random Locations

In this subsection, we evaluate the average BER performance of our proposed APC, GRPA, FPA, and TDMA.

We assume that the PD receiver is randomly located on the Ceiling. We randomly selected 30 points from the Receiver Plane as the PD receiver’s locations to simulate their average BER performance. For two LED transmitters scenario, three LED transmitters scenario, and four LED transmitters scenario, the simulation results are illustrated by Figures 4b and 5a,b, respectively. From the three figures, we can observe that the APC strategy we proposed can obtain best BER performance among the four schemes. In addition, the FPA scheme and GRPA scheme can hardly be applied to our considered uplink NOMA VLC system.

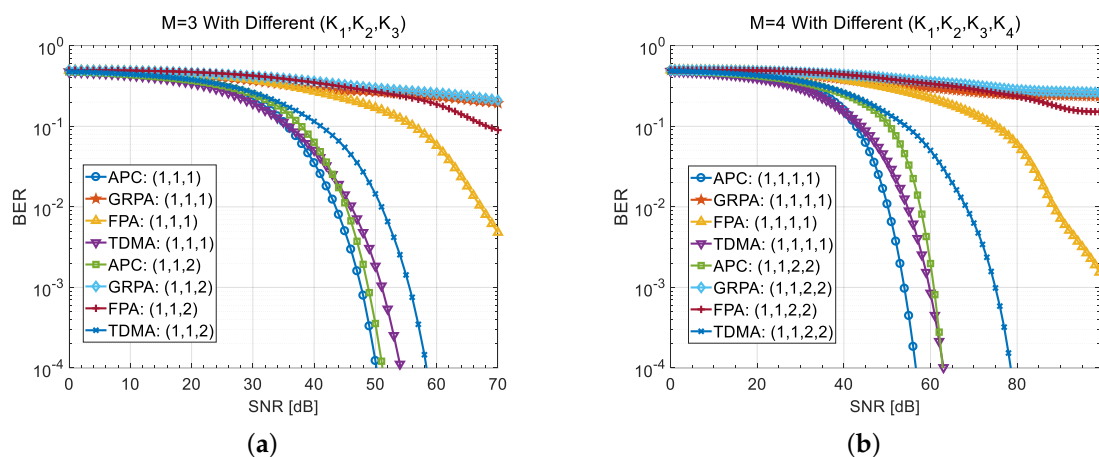


**Figure 5.** (a) Three users’ average BER performance comparisons of our proposed APC, GRPA, FPA and TDMA for different  $(K_1, K_2, K_3)$ ; (b) Four users’ average BER performance comparisons of our proposed APC, GRPA, FPA, and TDMA for different  $(K_1, K_2, K_3, K_4)$ .

### 5. Conclusions

In this paper, intended for an equivalent uplink NOMA VLC system, we have developed a channel and bit adaptive power control strategy to enhance the system’s energy-efficiency by jointly considering the channel state information and the transmission bit rate of each LED transmitter. Thanks

to the nice structure of the received constellation under our proposed APC strategy, we have proposed a low-complexity ML demodulation and decoding algorithm. Comprehensive computer simulation results have demonstrated that our proposed APC strategy significantly outperforms GRPA, FPA, and TDMA schemes.

**Author Contributions:** Z.-Y.W. has contributed in the conception and design of the study. Z.-Y.W., H.-Y.Y. have designed the experiments. Z.-Y.W. has written the paper. D.-M.W. has critically reviewed the paper. All authors have read and approved the final manuscript.

**Funding:** This work was supported in part by National Natural Science Foundation of China under Grant 61701536, in part by Guangdong Province Science and Technology Planning Project of China under Grant 2017B010114002 and in part by Dongguan Xinda Institute of Integrated Innovation.

**Conflicts of Interest:** The authors declare no conflict of interest.

## References

1. Komine, T.; Nakagawa, M. Fundamental analysis for visible-light communication system using led lights. *IEEE Trans. Consumer Electron.* **2004**, *50*, 100–107. [[CrossRef](#)]
2. O'Brien, D.C.; Zeng, L.; Le-Minh, H.; Faulkner, G.; Walewski, J.W.; Randel, S. Visible light communications: Challenges and possibilities. In Proceedings of the 2008 IEEE 19th International Symposium on Personal, Indoor and Mobile Radio Communications, Cannes, France, 15–18 September 2008; pp. 1–5.
3. Elgala, H.; Mesleh, R.; Haas, H. Indoor optical wireless communication: Potential and state-of-the-art. *IEEE Commun. Mag.* **2011**, *49*, 56–62. [[CrossRef](#)]
4. Jovicic, A.; Li, J.; Richardson, T. Visible light communication: opportunities, challenges and the path to market. *IEEE Commun. Mag.* **2013**, *51*, 26–32. [[CrossRef](#)]
5. Gancarz, J.; Elgala, H.; Little, T.D.C. Impact of lighting requirements on vlc systems. *IEEE Commun. Mag.* **2013**, *51*, 34–41. [[CrossRef](#)]
6. Pešek, P.; Zvanovec, S.; Chvojka, P.; Bhatnagar, M.R.; Ghassemlooy, Z.; Saxena, P. Mobile User Connectivity in Relay-Assisted Visible Light Communications. *Sensors* **2018**, *18*, 1125. [[CrossRef](#)]
7. Myung, H.G.; Lim, J.; Goodman, D.J. Single carrier FDMA for uplink wireless transmission. *IEEE Veh. Technol. Mag.* **2006**, *1*, 30–38. [[CrossRef](#)]
8. Karunatilaka, D.; Zafar, F.; Kalavally, V.; Parthiban, R. LED Based Indoor Visible Light Communications: State of the Art. *IEEE Commun. Surveys Tuts.* **2015**, *17*, 1649–1678. [[CrossRef](#)]
9. Kim, S.M.; Baek, M.W.; Nahm, S.H. Visible light communication using TDMA optical beamforming. *EURASIP J. Wirel. Commun. Netw.* **2017**, *2017*, 56. [[CrossRef](#)]
10. Zhu, Y.J.; Wang, W.Y.; Xin, G. Faster-than-nyquist signal design for multiuser multicell indoor visible light communications. *IEEE Photonics J.* **2017**, *8*, 1–12. [[CrossRef](#)]
11. Zhang, Y.Y.; Yu, H.Y.; Zhang, J.K.; Zhu, Y.J. Signal-cooperative multilayer-modulated VLC systems for automotive applications. *IEEE Photonics J.* **2016**, *8*, 1–9. [[CrossRef](#)]
12. Saito, Y.; Kishiyama, Y.; Benjebbour, A.; Nakamura, T.; Li, A.; Higuchi, K. Non-Orthogonal Multiple Access (NOMA) for Cellular Future Radio Access. In Proceedings of the 2013 IEEE 77th Vehicular Technology Conference (VTC Spring), Dresden, Germany, 2–5 June 2013; pp. 1–5.
13. Saito, Y.; Benjebbour, A.; Kishiyama, Y.; Nakamura, T. System-level performance evaluation of downlink non-orthogonal multiple access (NOMA). In Proceedings of the 2013 IEEE 24th Annual International Symposium on Personal, Indoor, and Mobile Radio Communications (PIMRC), London, UK, 8–11 September 2013; pp. 611–615.
14. Ding, Z.; Yang, Z.; Fan, P.; Poor, H.V. On the performance of non-orthogonal multiple access in 5G systems with randomly deployed users. *IEEE Signal Process. Lett.* **2014**, *21*, 1501–1505. [[CrossRef](#)]
15. Benjebbour, A.; Saito, Y.; Kishiyama, Y.; Li, A.; Harada, A.; Nakamura, T. Concept and practical considerations of non-orthogonal multiple access (NOMA) for future radio access. In Proceedings of the 2013 International Symposium on Intelligent Signal Processing and Communication Systems, Okinawa, Japan, 12–15 November 2013; pp. 770–774.
16. Yin, L.; Wu, X.; Haas, H. On the performance of non-orthogonal multiple access in visible light communication. In Proceedings of the 2015 IEEE 26th Annual International Symposium on Personal, Indoor, and Mobile Radio Communications (PIMRC), Hong Kong, China, 30 August–2 September 2015; pp. 1354–1359.

17. Marshoud, H.; Kapinas, V.M.; Karagiannidis, G.K.; Muhaidat, S. Non-orthogonal multiple access for visible light communications. *IEEE Photonics Technol. Lett.* **2016**, *28*, 51–54. [[CrossRef](#)]
18. Yang, Z.; Xu, W.; Li, Y. Fair non-orthogonal multiple access for visible light communication downlinks. *IEEE Wirel. Commun. Lett.* **2017**, *6*, 66–69. [[CrossRef](#)]
19. Marshoud, H.; Muhaidat, S.; Sofotasios, P.C.; Hussain, S.; Imran, M.A.; Sharif, B.S. Optical Non-Orthogonal Multiple Access for Visible Light Communication. *IEEE Wirel. Commun.* **2018**, *25*, 82–88. [[CrossRef](#)]
20. Huang, H.; Wang, J.; Wang, J.; Yang, J.; Xiong, J.; Gui, G. Symbol error rate performance analysis of non-orthogonal multiple access for visible light communications. *China Commun.* **2017**, *14*, 153–161. [[CrossRef](#)]
21. Wang, Z.Y.; Yu, H.Y.; Wang, D.M. Energy Efficient Transceiver Design for NOMA VLC Downlinks with Finite-Alphabet Inputs. *Appl. Sci.* **2018**, *8*, 1823. [[CrossRef](#)]
22. Moreira, A.J.C.; Valadas, R.T.; de Duarte, A.M. Performance of infrared transmission systems under ambient light interference. *IEE Proc. Optoelectron.* **1996**, *143*, 339–346. [[CrossRef](#)]
23. Boucouvalas, A.C. Indoor ambient light noise and its effect on wireless optical links *IEE Proc. Optoelectron.* **1996**, *143*, 334–338. [[CrossRef](#)]
24. Ghassemlooy, Z.; Alves, L.; Khalighi, M.; Zvanovec, S.; Uysal, M. *Visible Light Communications: Theory and Applications*; CRC Press: Boca Raton, FL, USA, 2017. ISBN: 9781498767538.
25. Kahn, J.M.; Barry, J.R. Wireless infrared communications. *Proc. IEEE* **1997**, *85*, 265–298. [[CrossRef](#)]
26. Shen, H.; Wu, Y.F.; Xu, W.; Zhao, C.M. Optimal power allocation for downlink two-user non-orthogonal multiple access in visible light communication. *J. Commun. Inf. Netw.* **2017**, *2*, 57–64. [[CrossRef](#)]
27. Xu, K.; Yu, H.; Zhu, Y. Channel-Adapted Spatial Modulation for Massive MIMO Visible Light Communications. *IEEE Photonics Technol. Lett.* **2016**, *28*, 2693–2696. [[CrossRef](#)]
28. Wang, Z.Y.; Yu, H.Y.; Zhang, Y.Y.; Wang, D.M. Optimization of Finite-Alphabet Signaling for Two-User Multiaccess VLC Systems. *IEEE Photonics J.* **2018**, *10*, 1–12. [[CrossRef](#)]
29. Boucouvalas, A.C. Asymmetry of free space optical links. In Proceedings of the SPIE on All optical Communication Systems: Architecture, Control and Network Issues, Philadelphia, PA, USA, 25–26 October 1995; pp. 69–76
30. Boucouvalas, A.C.; Barker, P. Asymmetric throughput in IrDA links. *IEE Colloquium Opt. Wirel. Commun.* **1999**, *7/1–7/5*:19990698. [[CrossRef](#)]
31. Boucouvalas, A.C.; Barker, P. Asymmetric throughput in optical wireless links. In Proceedings of the 2nd Electronic Circuits and Systems Conference, Bratislava, Slovakia, 6–8 September 1999; pp. 129–134.
32. Boucouvalas, A.C.; Barker, P. Asymmetry in optical wireless links. *IEE Proc. Optoelectron.* **2000**, *147*, 315–321. [[CrossRef](#)]
33. Zhang, Y.Y.; Yu, H.Y.; Zhang, J.K. Block Precoding for Peak-Limited MISO Broadcast VLC: Constellation-Optimal Structure and Addition-Unique Designs. *IEEE J. Sel. Areas Commun.* **2018**, *36*, 78–90. [[CrossRef](#)]
34. Cai, H.B.; Zhang, J.; Zhu, Y.J.; Zhang, J.K.; Yang, X. Optimal Constellation Design for Indoor  $2 \times 2$  MIMO Visible Light Communications. *IEEE Commun. Lett.* **2016**, *20*, 264–267. [[CrossRef](#)]
35. Zhu, Y.J.; Liang, W.F.; Zhang, J.K.; Zhang, Y.Y. Space-Collaborative Constellation Designs for MIMO Indoor Visible Light Communications. *IEEE Photonics Technol. Lett.* **2015**, *27*, 1667–1670.

